IEEE Access
Multidisciplinary | Rapid Review | Open Access Journal

Received August 26, 2019, accepted September 11, 2019, date of publication September 23, 2019, date of current version October 3, 2019.

Digital Object Identifier 10.1109/ACCESS.2019.2942968

Distribution Characteristics of Fragments Size and Optimization of Blasting Parameters Under Blasting Impact Load in Open-Pit Mine

XIAOHUA DING[1,2], WEI ZHOU[1,2], XIANG LU[1,2], MING LI[3], EBELIA MANDA[1,4], XUYANG SHI[1,2], BOYU LUAN[1,2], AND CHONGCHONG QI[5]

[1]School of Mines, China University of Mining and Technology, Xuzhou 221116, China
[2]State Key Laboratory of Coal Resources and Safe Mining, China University of Mining and Technology, Xuzhou 221116, China
[3]State Key Laboratory for Geomechanics and Deep Underground Engineering, China University of Mining and Technology, Xuzhou 221116, China
[4]School of Mines and Mineral Sciences, Copperbelt University, Kitwe 21692, Zambia
[5]School of Resources and Safety Engineering, Central South University, Changsha 410083, China

Corresponding authors: Wei Zhou (zhw19820624@163.com) and Xiang Lu (xianglu@cumt.edu.cn)

This work was supported in part by the National Natural Science Foundation of China under Grant 51804299 and Grant 51574222, and in part by the Natural Science Foundation of Jiangsu Province, China, under Grant BK20180646.

ABSTRACT The size distribution characteristics of fragments formed after loose blasting in open-pit mine will directly affect the economic benefits of the mining enterprise. The impact load test of coal samples with pressure ranging from 0.13MPa to 2.0MPa was carried out by using the split Hope Pressure Bar Test System (SHPB). Based on the theory of stress wave attenuation, the relationship between blasting load and coal samples impact test in the laboratory is established. It is concluded that with the increase of impact pressure, the degree of coal samples breakage increases gradually. According to the requirement of blasting quality in open-pit mine, it is concluded that the impact pressure range with good crushing effect is $0.30\text{MPa} \leq P \leq 0.90\text{MPa}$. Based on image recognition method, the fragmentation distribution characteristics of loose deposits of coal seam blasting in open-pit mine are obtained. Combining the impact load test in the laboratory and the fragmentation distribution of coal seam blasting, the influence area of blasting impact fragmentation is divided. According to the research results, two optimization schemes of blasting parameters are put forward and the blasting effect of the two schemes is verified by numerical simulation using ANSYS/LSDYNA. Through field blasting optimization test in open-pit mine, it is concluded that increasing blasting hole spacing and row spacing can effectively control dust pollution and increase massive coal rate.

INDEX TERMS Open-pit mine, fragments size distribution, impact load, numerical simulation, blasting optimization.

I. INTRODUCTION

The mining industry, especially the open-pit mining, are encountering many challenges, such as the proper waste disposal and improvement in efficiency [1]–[4]. Loose blasting to break coal and rock is one of the important ways of efficient mining in open pit coal mine [5]. In the mining process, fragmentation of coal and rock is an important index for evaluating blasting effect. It directly affects the blasting scheme, excavation and transportation equipment selection and economic effect of mining, and even seriously threatens the continuous safe production of mines [6]. Blasting fragmentation refers to the size of coal and rock fragments formed by blasting, and the specific evaluation indexes include fragments size distribution function, average size of fragments, the number of fragments in each size range [7]. The size distribution of blasting fragments is directly related to the production quality of mining engineering. A moderate degree of blasting fragmentation and the avoidance of producing huge blocks and excessive powdery particles are the basic requirements of mine blasting, which guarantees the best technical and economic results [8], [9]. Because of the complexity of blasting process and physical and mechanical properties of blasted rock mass, it is difficult to accurately predict the size

The associate editor coordinating the review of this manuscript and approving it for publication was Zhixiong Peter Li.

(a) Coal block with diameter d>300mm (b) Dust pollution

FIGURE 1. Coal seam blasting site in Ha'erwusu Coal Mine, China.

and distribution of rock mass fragmentation under blasting impact [10]. There are many factors affecting the quality of blasting fragmentation, which can be summarized into three aspects: rock physical and mechanical properties, blasting mode and blasting parameters [11], [12].

Due to a large number of cracks inside the coal seam, the size of the coal block after blasting is uneven. If the volume of the fragments is too large or too small after blasting, it will directly affect the cost of the coal mine. Using the Ha'erwusu Open-pit coal mine as an example, when the blasting intensity is low, the lump coal generated after blasting is too large, the secondary crushing cost increases, and the handling difficulty increases, as shown in Fig.1(a); at high altitude, the lump coal produced is too small, and the number of dust increases, as shown in Fig.1(b). This seriously affects the mine operating environment and corporate image, and limits the sustainable development capability of coal mines. These two aspects significantly restrict the environmental and economic benefits of open-pit mines. Therefore, the selection of appropriate blasting parameters and blasting methods can effectively solve the problems of high cost of secondary crushing in open-pit mines, difficulty in handling, and dust pollution generated from mine blasting and other major problems due to inefficient blasting.

The analysis of the block distribution characteristics is based on the statistics of the coal mine volume under each blasting process after the coal seam blasting. Based on the characteristics of the coal seam blasting block distribution, the blasting parameters are adjusted to effectively control the blasting block degree. Thus, the optimum size of coal block can be increased, the cost of secondary handling and crushing can be reduced, and the proportion of dust particles can be effectively controlled so as to achieve the goal of effective control of dust pollution in blasting. Focusing on the characteristics of coal seam blasting under existing blasting parameters, combined with the mechanical test of coal and rock under indoor impact load, the relationship between blasting parameters and block distribution is established. Based on the evaluation of blasting fragmentation characteristics, an optimization scheme of blasting parameters for controlling fragmentation distribution is proposed.

II. LABORATORY IMPACT TEST OF COAL SAMPLES

Split Hopkinson Pressure Bar (SHPB) is the most widely used method for testing the physical and mechanical properties of materials at high strain rates [13]. SPHB test is an important part of impact dynamics experiment. It can not only realize simple loads with high strain rate, but also form dynamic loads composed of various loads, such as active and passive confinement pressure [14]. SHPB experimental device can be applied to the field of blasting [15]. The experimental method is to indirectly promote the stress-strain relationship of sample material by measuring the strain on the impact prop. This is an indirect and simple experimental method [16]. Dai *et al.* conducted a quantitative study on the effect of protective materials for blasting damage of tunnel surrounding rock through SHPB test device [17]. Shi *et al.* used SHPB device to study the damaging effect of directional shock absorption blasting on rock [18]. Guo *et al.* made dynamic impact experiments on rock samples by means of Hopkinson pressure bar, and obtained the effective energy consumption needed for rock fragmentation [19]. It can be seen that SHPB experimental technology has been relatively mature in the study of dynamic mechanical characteristics of coal, and has been widely used in the field of blasting. The focus of the existing research results is to study the dynamic mechanical characteristics and failure characteristics of coal at different speeds, but little research has been done on the size of coal fragmentation under different impact loads, and the fragmentation of coal blasting will directly affect the economic benefits of mining enterprises. Therefore, the SHPB experimental technology is used to carry out dynamic impact tests of coal samples at different atmospheric pressures to study the relationship between impact load and coal fragmentation.

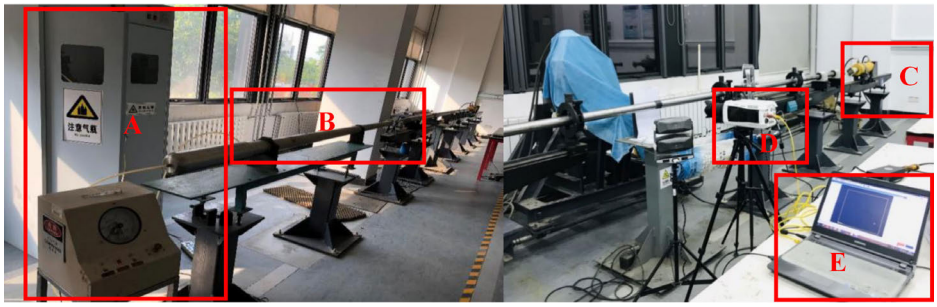

FIGURE 2. Test equipment and sample loading method.

FIGURE 3. Processed coal sample.

Using the SHPB test system of China University of Mining and Technology, the dynamic impact test of coal samples taken at different strain rates was carried out to study the relationship between impact load and the size of broken coal. The blasting scheme is the basis for this test.

A. TEST EQUIPMENT AND SAMPLE PREPARATION

The experiment adopts the φ 50mm SHPB test system of the State Key Laboratory of Geotechnical Mechanics and Underground Engineering of China University of Mining and Technology. The whole system includes five parts: load drive system(Fig.2 A), pressure bar system(Fig.2 B), energy absorption system(Fig.2 C), signal acquisition system(Fig.2 D) and signal processing system(Fig.2 E). The sample is placed between the entrance rod and the transmission rod.

The coal samples collected in this test were taken from the Ha'erwusu Open-pit coal mine in Erdos City, Inner Mongolia Autonomous Region, in China. The sample preparation was completed at the Mechanics Test Center of China University of Mining and Technology. The three processes of coring, cutting and grinding were used to complete the test coal samples. The sample size is 50mm high and 50mm diameter cylinder. The finished sample is shown in Fig.3.

B. TEST IMPACT LOAD DETERMINATION

The design and implementation of rock mechanics test under indoor impact load are mainly divided into three processes. Firstly, the minimum load value of coal sample damage is obtained by multiple impact load test. Secondly, the load is increased sequentially based on the minimum load. The impact load test is carried out. Finally, the failure characteristics of the sample after coal rock failure under different loads are analyzed, and the block distribution characteristics are determined. The results were compared with the distribution characteristics of coal seam blasting in an open-pit mine, and the degree of fragmentation in different blasting area was determined.

Through repeated tests, the minimum loading pressure that can cause the failure of the coal sample is 0.13MPa. The SHPB test system used in this test has a maximum loading pressure of 2.0MPa, therefore, 0.13MPa and 2.0MPa are used as the vertical load reference to design the impact load. Ten sets of impact tests were designed, and the impact loads were 0.13MPa, 0.17MPa, 0.25MPa, 0.30MPa, 0.50MPa, 0.70MPa, 0.90MPa, 1.20MPa, 1.50MPa, 2.0MPa, respectively. The sample was subjected to a dynamic compression test. Five samples of each group were tested under pressure and their mean values were taken as the impact crushing test results under this pressure.

C. COAL SAMPLE IMPACT FAILURE CHARACTERISTICS

In order to quantitatively study the influence of the impact load on the fracture characteristics of coal samples, the distribution law of fracture degree of coal samples under different impact loads is compared and analyzed. The average particle size δ of the test piece is used as the parameter to evaluate the failure characteristics. The coal samples are sieved and weighed by the grading sieve and the electronic balance. The block analysis method is used to calculate the average of the different test pieces. The particle size δ is used to investigate the influence of different impact loads on the average particle size δ of coal samples.

The pore size of the sieve selected from the test is specifically 15.0 mm, 10.0 mm, 5.0 mm, 2.0 mm, and 1.0 mm. The sample was sieved by using a grading sieve to obtain 6 sets of coal samples having particle diameters ranging from 15.0 to 50.0 mm, 10.0-15.0 mm, 5.0 to 10.0 mm, 2.0 to 5.0 mm, 1.0 to 2.0 mm, and 0.0 to 1.0 mm. According to the particle size, the number is i = 1,2,3...6 arrangement from large to small.

Using the analysis method of the above-mentioned block distribution characteristics, the crushed coal sample after the Hopkinson pressure bar test is classified and sieved.

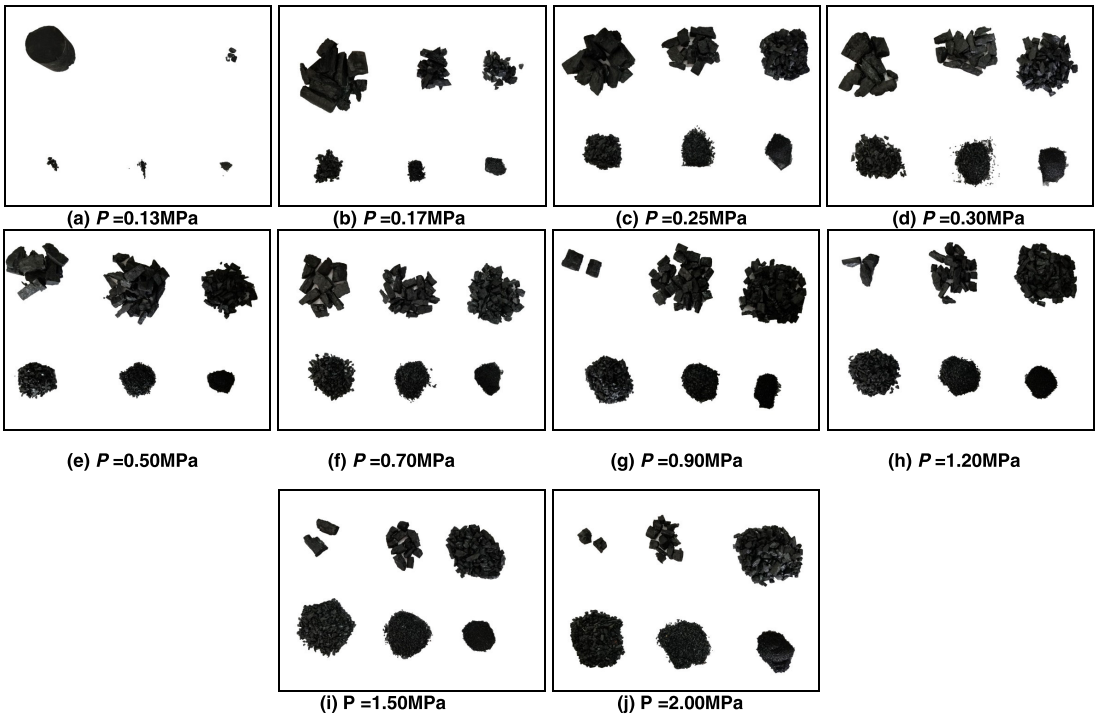

FIGURE 4. Characteristics of coal-like fragments after screening at various pressures.

TABLE 1. Characteristics of block distribution after coal sample failure under different pressures.

P/MPa	M_c/g	m_{iv}/%						δ/mm
		i=1	i=2	i=3	i=4	i=5	i=6	
0.13	359.1	98.93	0.00	0.68	0.27	0.07	0.05	32.21
0.17	356.4	74.98	15.52	6.12	2.10	0.81	0.47	27.63
0.25	366.9	49.99	24.09	14.51	6.13	3.69	1.59	21.83
0.30	354.6	37.14	34.98	15.16	6.84	4.22	1.66	19.64
0.50	362.4	32.52	30.12	21.15	9.02	4.98	2.21	17.83
0.70	365.4	30.25	25.26	26.02	11.87	4.79	1.81	16.70
0.90	365.4	10.27	35.43	31.23	15.65	6.47	2.95	12.54
1.20	360.3	9.07	23.33	30.07	20.32	14.14	3.07	10.22
1.50	382.5	10.30	15.99	32.11	21.37	15.71	4.52	9.56
2.00	396.9	4.65	14.68	29.63	18.26	23.33	9.45	7.34

As shown in Fig.4, with the loading impact pressure increasing from 0.13MPa to 2.00MPa, the degree of coal sample fragmentation is gradually intensified, and the proportion of large-sized blocks in coal-like fragments is gradually decreasing, while the proportion of small-sized fragments and powdered coal particles is gradually increasing, that is, the fragmentation of coal sample shows strong correlation of impact pressure.

From the analysis of the coal sample after the above impact damage, the mass percentage and average particle diameter of the fragments under impact pressure were obtained. See Table 1, where M_c is the total mass of the coal sample, and m_{iv} is the particle size of the i-group after the sample is destroyed. Based on the Quality as a percentage of total mass, the particle size distribution characteristics of the coal-like fragments and the variation of the average particle size with the impact pressure are analyzed, as shown in Fig.5.

The average particle size of the broken coal sample gradually decreased with the increase of air pressure, indicating that the degree of damage to the coal sample gradually increased.

D. COAL SAMPLE IMPACT DAMAGE BLOCK DISTRIBUTION EVALUATION

In order to further combine the test results with coal seam blasting in an open-pit mine, the particle size distribution of

TABLE 2. Distribution characteristics of coal and rock scale under various impact pressures.

Fragment scale	Fragment mass percentage m_{iv}/% at each pressure P/MPa									
	0.13	0.17	0.25	0.30	0.50	0.70	0.90	1.20	1.50	2.00
Large diameter	98.93	74.98	49.99	37.14	32.52	30.25	10.27	9.07	10.30	4.65
Medium diameter	0.95	23.74	44.73	56.98	60.29	63.15	82.31	73.72	69.47	62.57
Powder	0.12	1.28	5.28	5.88	7.19	6.60	9.42	17.21	20.23	32.78

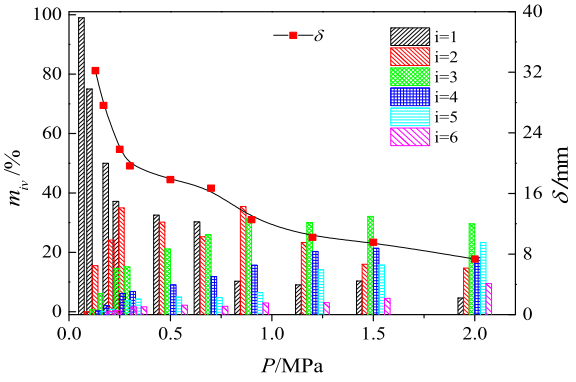

FIGURE 5. The variation of particle size distribution and average particle size of coal sample with impact pressure.

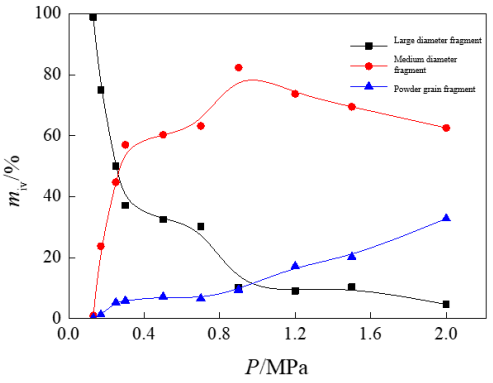

FIGURE 6. Curve of mass fraction of different scales with pressure.

coal and rock under the impact of indoor impact is further divided.

According to the block distribution characteristics of coal rock sample failure under impact load, combined with the minimum cost control of coal seam blasting, the broken pieces are divided into three groups according to the particle size range: large diameter, medium diameter and powder. The particle size ranges corresponding to the three groups of fragments are:

1) Large diameter fragments: particle size $d \geq 15.0$mm, that is, $i = 1$ group of fragments. The size of this group of fragments is relatively large. In the Ha'erwusu Open-pit coal mine, the corresponding large-volume coal is required to be blasted after the corresponding coal seam blasting, with a coal diameter of 300 mm < d.

2) Medium diameter fragments: particle size 15.0mm $\geq d \geq$ 2.0mm, that is, $i = 2, 3, 4$ pieces. The size of the fragments in this group is moderate. If it corresponds to the size of the fragments after the blasting of the coal seam, then the fragments in the range do not need to be broken. Corresponding to massive coal, the coal diameter is 50mm $\leq$ d $\leq$ 300mm.

3) Powder fragments: particle size 2.0mm $\geq d$, $i = 5$, 6 groups of particle size range fragments. The size of the group of fragments is relatively small, which corresponds to the small volume of coal after the blasting of the coal seam, even pulverized coal, which is the main source of blasting dust in the mine pit. Corresponding to granular coal, the coal diameter $d \leq 50$mm.

According to the above-defined method, the distribution characteristics of the fragments at different scales under the loading pressure of each group can be obtained, as shown in Table 2. Fig.6 shows the variation of the mass percentage of coal and rock fragments with the pressure at three sets of scales.

It can be seen from Fig.6 that as the gas pressure increases, the mass percentage of the fragments at each scale changes significantly. Specifically: with the increase of air pressure, the mass percentage of large-diameter fragments gradually decreases; for medium-diameter fragments, the mass percentage increases with air pressure, and the overall appearance shows an increasing change characteristic. When the gas pressure exceeds 0.90MPa, the mass percentage of the medium-diameter fragments has a decreasing variation characteristic, and the reduction amplitude is about 20%; compared with the variation characteristics of the mass percentage of the other two groups of scales, the mass percentage of the powder fragments and the increase in air pressure is approximately linear.

It can be seen from the analysis of Table 2 and Fig.6 that increasing the impact gas pressure can effectively reduce the mass percentage of the large diameter fragments, thereby reducing the amount of secondary broken coal and controlling the secondary crushing input cost. However, as the air pressure increases, the mass percentage of the powder fragments gradually increases, which will greatly increase the investment in coal mine dust suppression costs. According to the requirement of coal fragmentation quality standard in the

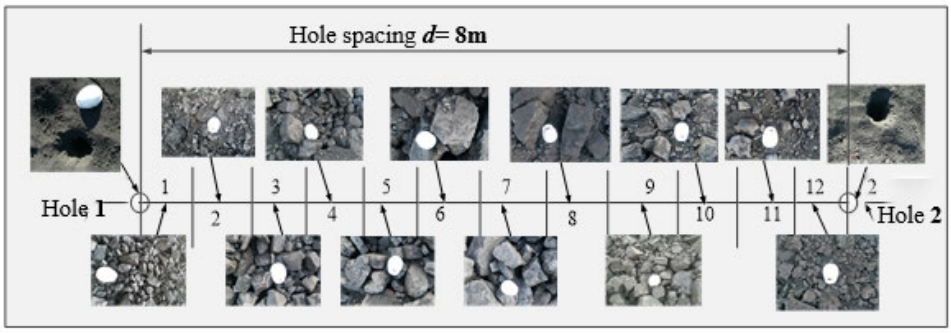

FIGURE 7. Blast block image picking scheme between holes.

open-pit coal mine, after coal seam blasting, the proportion of massive coal should be increased as much as possible, the proportion of granular coal should be reduced, and the proportion of large volume coal that can be broken twice should be controlled. From this, it can be concluded that the range of good fragmentation effect in the test is: the proportion of large diameter fragments is less than 40%; the proportion of medium diameter fragments is more than 50%; the proportion of powder fragments is less than 10%. According to the above quality control standards, compared with the data in Table 2 , it is concluded that the impact pressure of coal rock is the best in the range of 0.30Mpa $\leq$ P $\leq$ 0.90MPa.

III. MATHEVALUATION OF BLASTING EFFECT OF HA'ERWUSU OPEN-PIT MINE

The coal seam blasting of a certain Ha'erwusu open-pit mine was selected as the fragmentation distribution observation area. The whole blasting area is 345m in length and 45m in width. The blasting bench height is 8m, the blasting volume is 115200m^3, the weight of explosive used is 24.3t, the blasthole depth is 9m, the blasthole spacing is 8m, the row spacing is 6m, and the number of blastholes is 300. In the direction of the blasting area length, the holes are equally spaced. Assuming that the coal quality in the whole blasting area is uniform, the failure characteristics and fragmentation distribution characteristics of coal and rock between every two holes in the long direction are the same. Therefore, the area between any two groups of blastholes is selected for blasting block analysis. According to the requirement of photographic frame and image sharpness, it is divided into 12 equal spacing image pickup regions within 8 m hole spacing, as shown in Fig.7.

A. EXPLOSION BLOCK DEGREE CLASSIFICATION IMAGE RECOGNITION

After the blasting of coal and rock, the block size and distribution range are large. The large-size grading screen and the matching excavator are used, which has a large workload [20]–[22]. The development of an intelligent classification system based on image recognition (such as the shape, color, size, etc. of the material) can improve work efficiency and has many advantages over manual screening, such as uniform grading standards, reduction of mechanical noise and energy consumption, as well as providing statistical information on various classification indicators [23]–[25].

The rock mass degree intelligent grading system is written by MATLAB software [26], [27]. MATLAB's image processing toolbox contains many image processing related functions that can be easily applied to digital image programming [28]–[31]. The image processing program of coal and rock block after blasting includes:

1) Image import: Use the imread function to import the live image into matlab, as shown in Fig.8(a).

2) Image enhancement: imadjust is used to enhance the gray level of the image. The histeq function equalizes the image histogram, and uses medfilt2 to median the image to remove noise and black spots in the image, as shown in Fig.8(b).

3) Determining the rock mass interface: Using the gradient magnitude as the segmentation function, the Sobel edge concealment, the Imfilter function, and some simple algorithms are used to calculate the gradient magnitude, as shown in Fig.8(c).

4) Image binarization: Separate the rock blocks in the image by using the rock boundary line obtained above, then transform the gray image into a binarized image by using the im2bw function, and the bwareaopen function is used to remove the small rocks and flaws in the graph, see Fig.8(d).

5) Setting of the reference object: A helmet with a diameter of 0.2 m is placed in the image for calibrating the size of the rock in the image, as shown in Fig.8(e).

6) Rock block identification: The connected area in the image is identified by the bwconncomp function, and the identified image is as shown below. The block marked by the red hexagonal star is a helmet, see Fig.8(f).

7) Block grading: Firstly, the regionprops function is used to calculate the properties of the connected regions, and then the bar function is used to classify the coal briquettes.

Through the image recognition method, the coal blocks in different blasting areas between the two blastholes are divided into four groups of sizes of 0.0-50mm, 50-200mm,

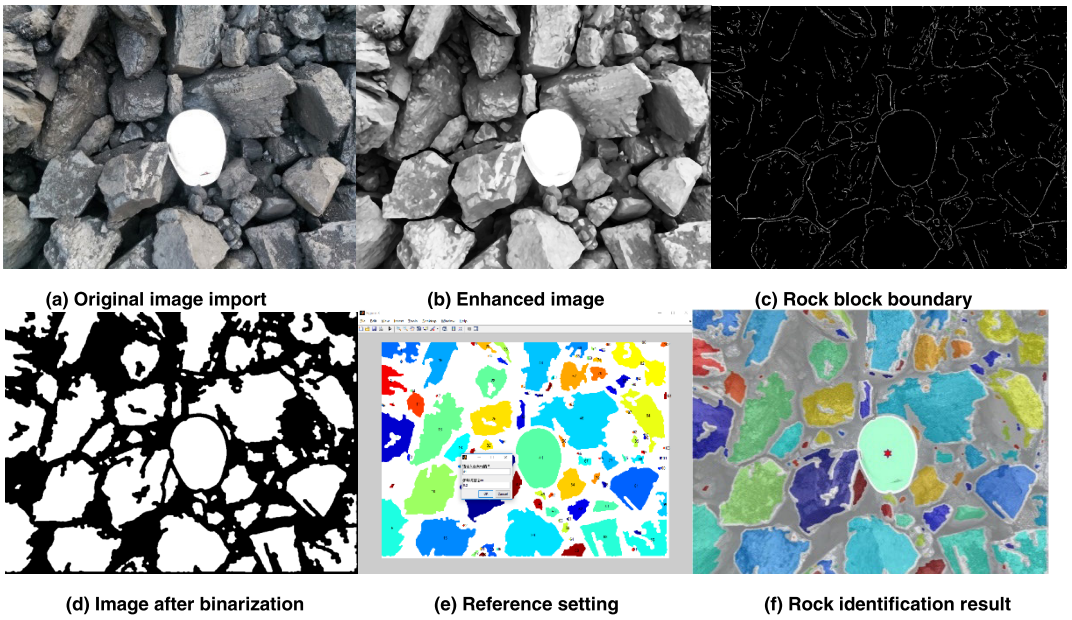

FIGURE 8. Coal rock block image processing program.

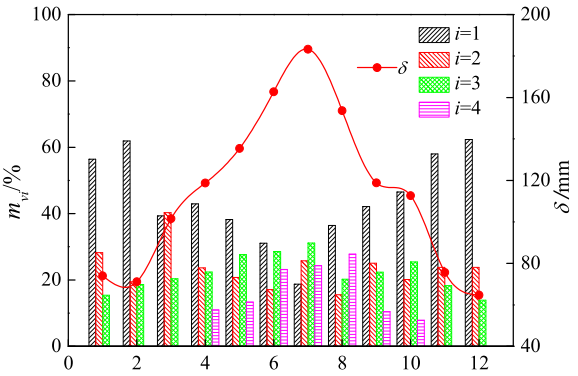

FIGURE 9. Variation of coal blasting block degree and the average size of coal block.

200-300mm and more than 300mm, and they are numbered i = 1 and 2 according to the size from large to small 3, 4. Table 3 shows the variation of the mass percentage of the coal mass (percentage of each particle size in the image) and the average size in each area between the two blastholes. The variation curve of coal seam blasting block size and average coal block size in each area is shown in Fig.9.

According to the division method of each region in Fig.9, the smaller the region number, the closer the region is to the blasthole 1. As the region number increases, the observation region gradually moves away from the blasthole 1, and gradually approaches the blasthole 2, and the observation region 6, 7 is the middle position of the two groups of blastholes, that is, the farthest observation area from the blasthole.

It can be seen from Table 3 and Fig.9. As the distance from the blasthole increases, the large-size fragments first increase and then decrease, and the small-size fragments decrease first and then increase. The particle size δ of the fragment first increases and then decreases. It can be concluded that the closer to the two blastholes, the more severe the damage of the coal and the smaller the particle size, and the farther away from the two blastholes, the greater the coal fragmentation.

B. EVALUATION OF BLASTING PROCESS PARAMETERS BASED ON BLOCK DEGREE DISTRIBUTION

According to the classification standard of coal blocks on section II, part D, the scale distribution characteristics of coal blocks in different blasting areas between the two blastholes after coal blasting can be obtained, as shown in Table 4. Fig.10 shows the mass percentage of coal masses with different scales between the two blastholes as a function of the observed area.

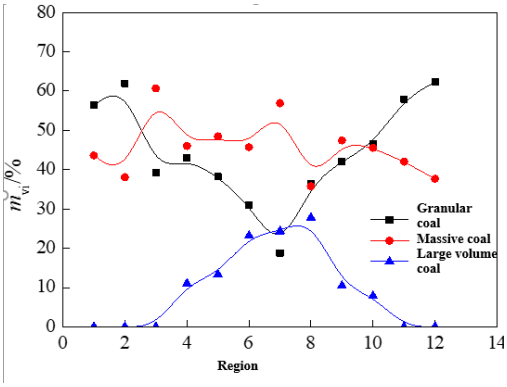

FIGURE 10. Characteristics of mass fraction of coal mass with different scales.

As can be seen from Fig.10, the mass percentage of the lump coal in each region is substantially above 40%, wherein the mass percentage of lump coal between the regions 2

TABLE 3. Block distribution and average size characteristics of coal after blasting in various areas between the blastholes.

Region	m_{vi} / %				δ/mm
	i=1	i=2	i=3	i=4	
1	56.38	28.25	15.37	0	73.99
2	61.92	19.46	18.62	0	71.13
3	39.32	40.29	20.39	0	101.59
4	42.97	23.66	22.39	10.98	118.74
5	38.21	20.78	27.68	13.33	135.42
6	31.09	17.12	28.59	23.2	162.73
7	18.76	25.77	31.14	24.33	183.30
8	36.44	15.55	20.21	27.8	153.61
9	42.13	25.08	22.35	10.44	118.80
10	46.54	20.14	25.44	7.88	112.67
11	57.96	23.77	18.27	0	75.64
12	62.33	23.79	13.88	0	64.69

TABLE 4. Distribution characteristics of coal blocks in each blasting area.

Fragment types	Percentage of broken mass in each blasting area m_{vi} / %					
	1	2	3	4	5	6
Granular coal	56.38	61.92	39.32	42.97	38.21	31.09
Massive coal	43.62	38.08	60.68	46.05	48.46	45.71
Large volume coal	0	0	0	10.98	13.33	23.2
Fragment type	Percentage of broken mass in each blasting area m_{vi} / %					
	7	8	9	10	11	12
Granular coal	18.76	36.44	42.13	46.54	57.96	62.33
Massive coal	56.91	35.76	47.43	45.58	42.04	37.67
Large volume coal	24.33	27.8	10.44	7.88	0	0

and 10 is close to or exceeds 50%. As the large-volume coal moves away from the blasthole, the mass percentage increases slowly in a straight line. In numerical terms, the mass percentage of the large-volume coal is basically controlled within 30%. In the specific production, the amount of secondary crushing coal is acceptable. However, unlike the other two groups of coal mass variation characteristics, the mass percentage of granular coal gradually decreases with the distance from the blasthole, but even if it's minimum value is below 20%, the granular coal within 3m from the blasthole has its mass percentage even exceeds 40%, which will cause serious dust pollution to the pit.

On the whole, the existing coal seam blasting scheme can achieve the purpose of controlling the secondary blasting cost to a certain extent, but it cannot better control the number of coal blocks at the small scale, that is, the direct blasting dust pollution is more serious.

IV. BLASTING OPTIMIZATION TEST AND EFFECT EVALUATION OF HA'ERWUSU OPEN-PIT MINE

A. BLASTING PARAMETER OPTIMIZATION SCHEME

According to the fragmentation distribution characteristics of coal blasting in Ha'erusu open-pit mine, the optimization objectives of blasting parameters mainly include two aspects that reducing the mass percentage of granular coal and increasing the mass percentage of massive coal.

In the current coal seam blasting scheme, there are three main parameters that can be adjusted: the hole spacing d, the row spacing h, and the explosive quantity Q. Therefore, the optimization scheme of the blasting parameters is mainly carried out around these three parameters.

According to the *Safety Regulations for Blasting* [31] and the *Practical Manual for Engineering Blasting* [32], the calculation formula of the shock wave in blasting process of open-pit mine is:

$$\Delta P = \eta K(Q^{\frac{1}{3}}/R)^{\alpha} \tag{1}$$

In the formula, α and K are empirical coefficients, respectively 1.31, 0.67; η is the attenuation index through actual measurement. Through actual tests, the value is 0.71; Q is the charge, kg; R is the distance from a point in the coal seam to the centre of the explosive, m.

According to the data in Section III, the 300 blastholes in the coal seam blasting in the field observation area consume a total of 24.3 tons of explosives. According to the principle of average distribution, the explosive amount of each blasthole

TABLE 5. Single hole blasting affected area division.

Blasting area	Blasting range R	Blasting coal block scale
Crushing area	$R \leq 2.01$m	Granular coal
Broken damage zone	$2.01\text{m} \leq R < 4.63$m	Massive coal
Rupture zone	$4.63\text{m} \leq R < 8.78$m	Large volume coal
Undisturbed zone	$R \geq 8.78$m	——

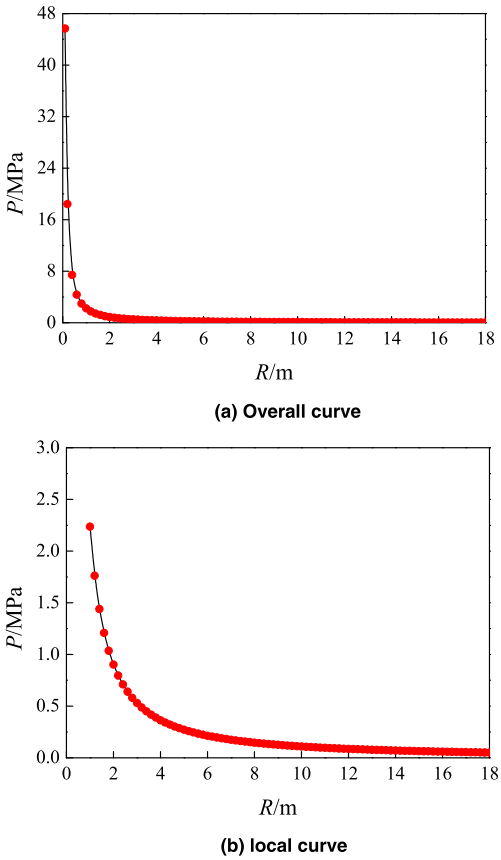

FIGURE 11. Curve of impact blasting load as a function of blasthole distance.

is $Q = 81$kg, and the Q value is substituted into the formula (1), which can be shown. The relationship between the air pressure P and the blasting distance R:

$$P = 0.71 \times 0.67 \times (81^{\frac{1}{3}}/R)^{1.31} \quad (2)$$

According to formula (2), the impact load versus blasting distance curve can be obtained, as shown in Fig.11.

It can be seen from Fig.11 that the stress wave generated by the explosion of the explosive is rapidly decayed in logarithmic form as it is far away from the blasting core. When the distance is greater than 8.8 m, the impact load is reduced to less than 0.1MPa. According to the test of the indoor impact load of the coal sample in the Ha'erwusu open-pit coal mine in Section II, the minimum load of the coal rock sample is 0.13MPa, which can be substituted into the formula (2) to obtain the distance between the rupture zone and the blasthole is $R_3 = 8.78$m; According to the evaluation of impact damage of the coal samples, the loading pressure is $0.30\text{MPa} \leq P \leq 0.90\text{MPa}$, and the coal-rock sample is mainly broken by the medium-diameter fragment, which can be solved to obtain the influence range of $2.01\text{m} \leq R \leq 4.63$m. Therefore, the blasting single hole affected area can be divided:

According to Table 5, the distribution and intersection of the blasting areas of the three blastholes in the triangle point can be determined. As shown in Fig.12, when considering the three blasthole explosion processes are independent of each other, the blasting areas of the three blastholes can be seen. The superposition relationship is very complicated, as shown in Fig.12(a). According to the rock, the load in the rupture zone is less than 0.3MPa. When the load in this zone is superimposed on the damage zone of another blasthole, the impact is limited. Therefore, the rupture zones of the three blastholes are removed, mainly looking at the other two zones. The superimposed features, as shown in Fig.12(b), under the current hole spacing and row spacing design, the fractured and damaged areas of the three blastholes have a large area overlap, and even there is an influence superposition area of three blastholes in a certain area. This has a significant impact on the degree of coal seam blasting, which is also the reason for the large mass percentage of granular coal.

Based on the theoretical calculation combined with the coal samples impact failure test and the fragmentation distribution characteristics of coal seam blasting, the blasting parameters optimization scheme is given for the coal seam mining area of Ha'erwusu open-pit mine: In the first scheme, the hole spacing is increased from 8m to 12m, the row spacing is increased from 6m to 7m, and the remaining blasting parameters are unchanged; In the second scheme, the amount of single-hole explosives is reduced from 81kg to 48kg, and the remaining blasting parameters are unchanged.

B. BLASTING AREA SUPERPOSITION RATIONALIZATION VERIFICATION SECTION

The blasting area according to the theoretical formula and experiment has been divided. This section will use the numerical simulation method to verify the blasting area optimization rationalization after the blasting parameters

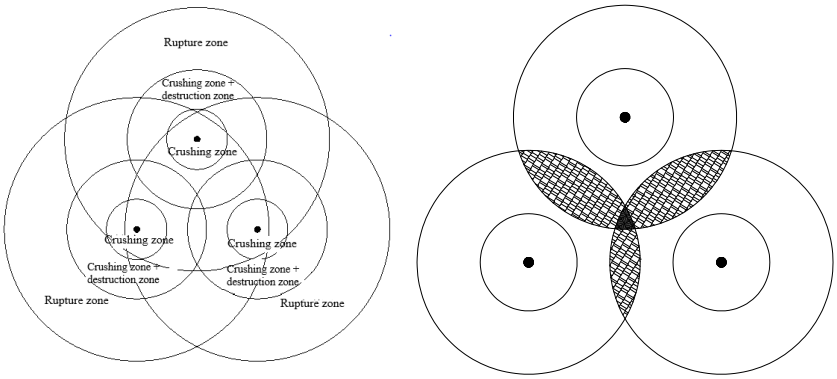

(a) Three-zone intersection (b) Two-zone intersection

FIGURE 12. Crossing characteristics of the damage zone after the blasthole triangle is arranged.

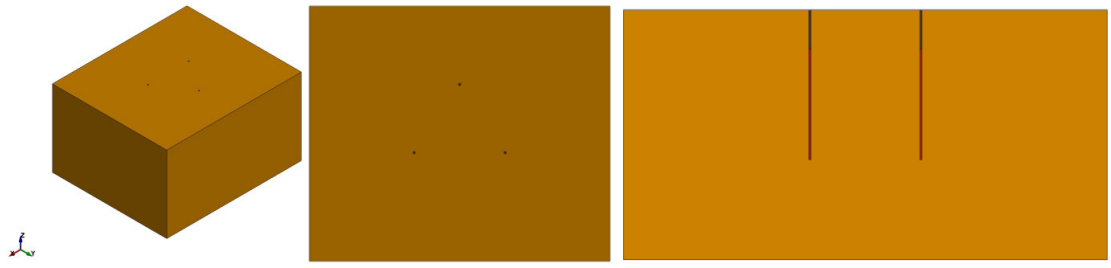

(a) Overall model (b) Top view (c) Two-hole profile

FIGURE 13. Meshing of the computational model.

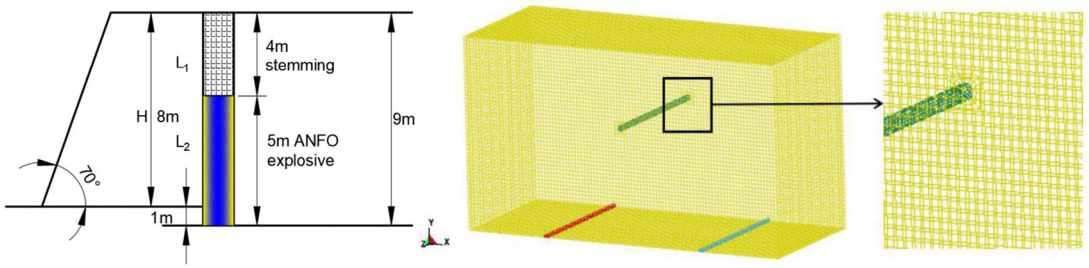

(a) Blasthole charge structure (b) Meshing of the numerical simulation model

FIGURE 14. Computational Model of Blasthole Charge Structure and Mesh Generation.

are optimized. The main contents are verified in two aspects: first, between the holes on whether the blasting area is uniformly affected by the stress wave; secondly, the crushing areas between the two holes can be connected to each other.

1) TEST METHOD

In the numerical simulation, ANSYS/LS-DYNA software is used to study the damage characteristics of adjacent boreholes after the explosion and the distribution characteristics of cracks in the damage zone [33], [34]. The process of establishing the model is extremely important and the quality of the model will directly affect the calculation results [35], [36]. In order to simplify the process of modelling and reduce the amount of repeated calculation, the number of simulated blasting holes is simplified to three, the arrangement is triangular, and the specific parameters such as the spacing of blasting holes and row spacing are set according to the actual blasting design of the mine. In the triangle range formed by blasting holes, the stress in the blasting process of small-scale blasting zone can be accurately simulated. The model uses 3DSOLID164 units, and the results can be extended to the whole boundary stress simulation results of blasting zone. According to the given parameters, a three-dimensional model is constructed and its meshes are divided into 81408 units. Fig.13 and Fig.14respectively give the calculation model and meshing of coal seam blasting analysis.

TABLE 6. Physical and mechanical properties of coal.

Density /（kg/m^3）	Compressive strength /MPa	tensile strength /MPa	Elastic Modulus /GPa	Poisson's ratio	Cohesion /MPa	Internal friction angle /°
1350	26.50	1.03	2.45	0.21	0.74	32

TABLE 7. Ammonium fry material parameters.

Density /（kg/m^3）	Detonation speed（m/s）	A/GPa	B/GPa	ω	R_1	R_2	Elastic Modulus /GPa
1050	4500	214.40	0.182	0.15	4.2	0.9	4.19

Note: A, B, R_1, R_2, ω are the explosive material constants

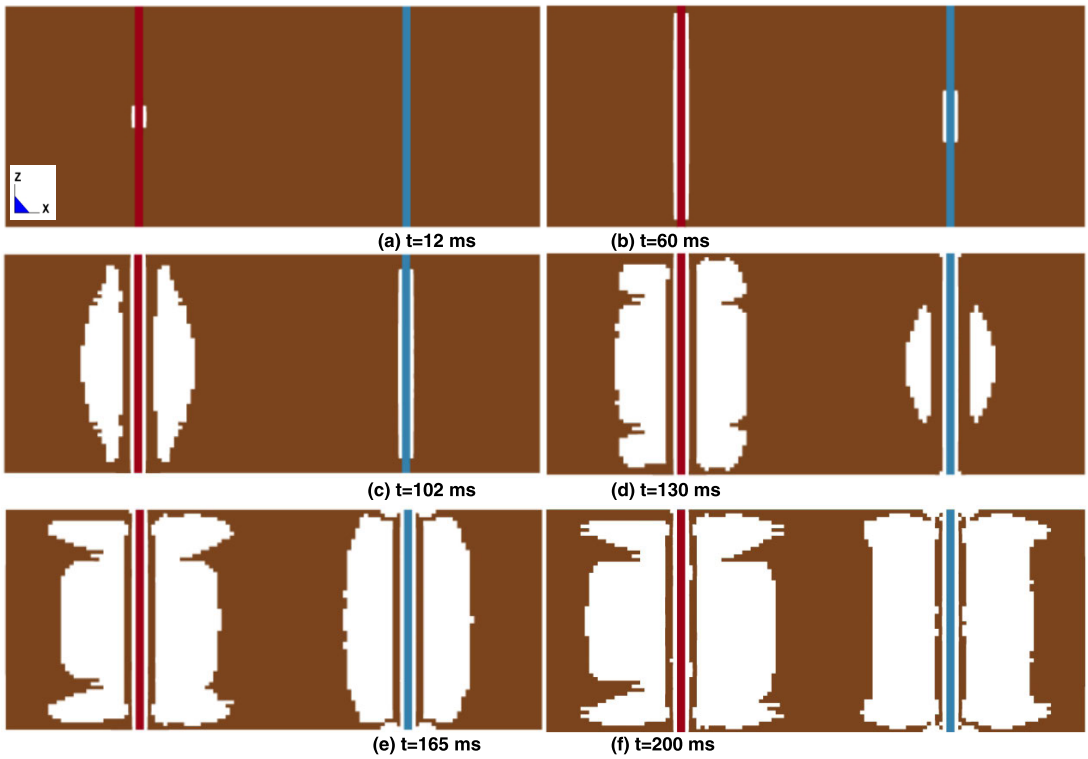

FIGURE 15. Development process of blasting rock fissures.

RHT concrete constitutive model has been widely used in numerical simulation of explosive impact. Based on the similarity between concrete and rock, the dynamic constitutive relationship of concrete can be used to describe the mechanical behavior of rock materials under dynamic loading. On the basis of fully considering the elastic limit surface, failure surface and damage softening equation, RHT concrete constitutive model is divided into three stages: elastic stage, linear strengthening stage and damage softening stage [37], [38]. Table 6 and Table 7 give the physical and mechanical parameters of coal and the material parameters of ANFO explosive during the numerical calculation.

The development process of rock fissures is simulated by ANSYS/LS-DYNA software. As shown in Fig.15, by observing the development process of rock fissures, it can be found that rock fissures extend from the centre of the borehole to the surrounding area. Because explosives are filled in the middle and lower parts of the borehole, the detonator first detonates the explosives in the middle part of the borehole. From Fig.15(a) and Fig.15(b), it can be concluded that the chemical reaction of the explosive has been transmitted to the whole hole for a very short time at the beginning of the explosion of 60ms. Fig.15(c) shows that fissures first develop in the middle of the borehole where the first explosive reaction occurs, and gradually expand to the top and bottom of the borehole, and finally the fissures cover the whole borehole. Due to millisecond blasting, an is shown in Fig.15(d), Fig.15(e) and Fig.15(f), the initiation of adjacent boreholes is delayed for a

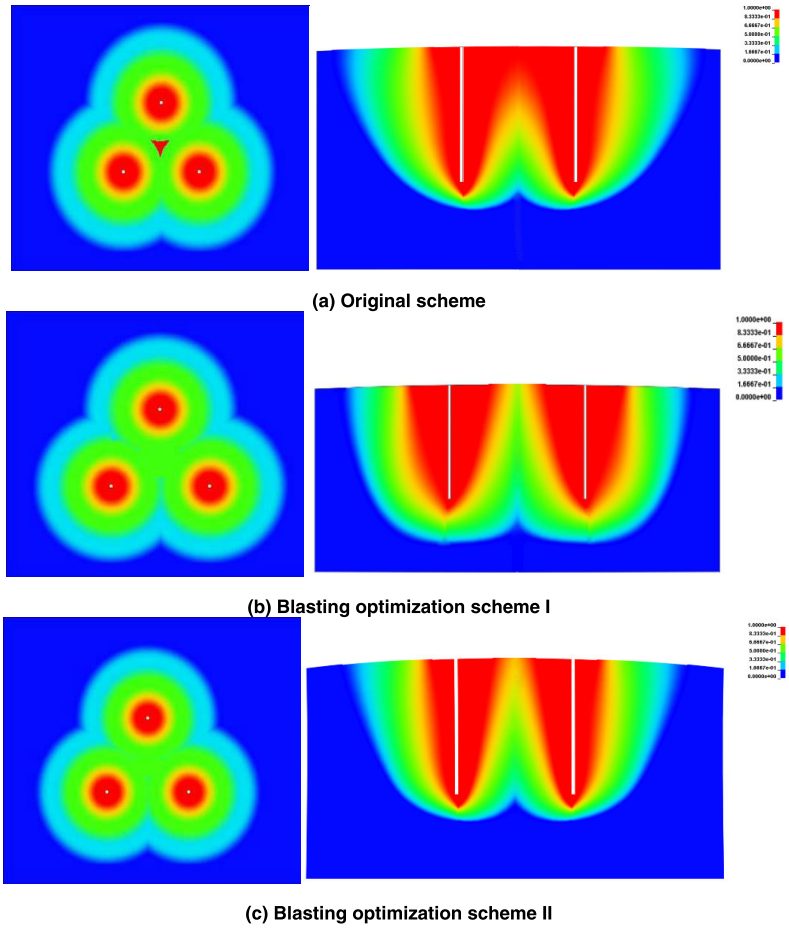

FIGURE 16. Damage characteristics of coal and rock in the blasting area around the blast hole.

certain time (42ms). When the second borehole is detonated, the rock crack damage along the diameter direction of the first borehole has basically developed, and the ultimate crack development range is the approximately cylindrical shape with the borehole as the axis.

Fig.16 shows the damage characteristics of coal seams within the influence range of the blasthole stress wave and the damage characteristics of coal and rock between the two blastholes under the current blasting scheme and two blasting optimization schemes. As can be seen from the figure, Under the current blasting scheme, the fracture and failure zones between the three holes are superimposed on each other, and the comminution zone is formed in the middle zone. Within the influence range of the single hole, each damage zone is basically funnel-shaped, and the two holes are broken. The simulation results are consistent with the cross characteristics of the damage zone in Section IV, part A, which shows that the stress distribution of the simulation results is consistent with the change curve of blasting impact load and hole spacing shown in Fig.11. Under the two optimization schemes, the coal damage characteristics in the surrounding area of each blasthole and in the intersection area are basically the same. The three-hole intersection area and the two-hole intersection area crushing and destruction area are connected to each other, and there is no crushing area formed by superimposing each other. Both optimization schemes can meet the optimization requirements. From the perspective of the utilization of the blasthole charge, the first scheme is superior to the second scheme, and the first scheme is selected as the final test scheme.

C. BLASTING OPTIMIZATION TEST AND BLOCK DISTRIBUTION CHARACTERISTICS

According to the theoretical verification of the coal seam blasting parameters optimization scheme, the coal seam blasting test was carried out in the Ha'erwusu open-pit coal mine. In this test, the spacing of the blastholes was increased from 8m to 12m in the original design, and the row spacing of the blastholes was increased from 6m to 7m. The other perforation methods and the parameters of the pyrotechnics were the same as the original blasting parameters.

Fig.17 shows the coal seam blasting site under optimized conditions. Similarly, the coal seam blasting area between

(a) Blasting effect of the original scheme

(b) Blasting optimization effect of scheme I

FIGURE 17. Coal seam blasting site under optimization scheme.

TABLE 8. Characteristics of block distribution after coal blasting in various areas between the blastholes under original scheme and optimized scheme.

Region	m_{vi} / %								δ/mm	
	i=1(0.0-50mm)		i=2(50-200mm)		i=3(200-300mm)		i=4(>300mm)			
	original	optimization	original	optimization	original	optimization	original	optimization	original	optimization
1	56.38	51.32	28.25	25.77	15.37	22.91	0	0	73.99	102.32
2	61.92	44.32	19.46	25.41	18.62	30.27	0	0	71.13	118.52
3	39.32	36.21	40.29	32.22	20.39	28.35	0	3.22	101.59	129.86
4	42.97	33.54	23.66	27.66	22.39	27.57	10.98	11.23	118.74	145.58
5	38.21	28.27	20.78	25.44	27.68	35.42	13.33	10.87	135.42	160.03
6	31.09	18.46	17.12	30.05	28.59	31.85	23.2	19.64	162.73	180.72
7	18.76	10.77	25.77	18.88	31.14	47.98	24.33	22.37	183.30	213.35
8	36.44	15.26	15.55	30.54	20.21	24.08	27.8	30.12	153.61	192.55
9	42.13	22.13	25.08	29.11	22.35	37.91	10.44	10.85	118.80	169.25
10	46.54	25.41	20.14	20.86	25.44	48.26	7.88	5.47	112.67	169.49
11	57.96	30.22	23.77	25.44	18.27	44.34	0	0	75.64	150.21
12	62.33	42.57	23.79	27.13	13.88	30.3	0	0	64.69	120.31

the two blastholes is divided into 12 regions (the span of each region under the optimized scheme is 1 m, and the span of each region under the original scheme is 0.67 m), and the digital image processing technology is used for the gun. The block distribution characteristics between the holes were analyzed.

Table 8 shows the distribution characteristics of coal seam blasting in the blasting area between two blastholes under the two conditions of the original scheme and the optimization scheme. It can be seen from the table that compared with the original scheme, the mass percentage of coal in the smallest particle size range is smaller than the corresponding value

TABLE 9. Distribution characteristics of coal blocks in each blasting area under optimization scheme.

Fragment type	Mass percentage of fragments in each blasting area m_{vi} / %					
	1	2	3	4	5	6
Granular coal	51.32	44.32	36.21	33.54	28.27	18.46
Massive coal	48.68	55.68	60.57	55.23	60.86	61.9
Large volume coal	0	0	3.22	11.23	10.87	19.64
Fragment type	Mass percentage of fragments in each blasting area m_{vi} / %					
	7	8	9	10	11	12
Granular coal	10.77	15.26	22.13	25.41	30.22	42.57
Massive coal	66.86	54.62	67.02	69.12	69.78	57.43
Large volume coal	22.37	30.12	10.85	5.47	0	0

under the original scheme in the same area under the optimization scheme, and the expansion of the inter-row spacing can effectively improve the overall block size of coal seam damage.

According to the standard of coal block grading after coal blasting given in section II, part D, the distribution characteristics of coal blocks in each analysis area after optimization scheme are given, as shown in Table 9, except for the area within 2m from the blasthole, in other areas the mass percentage of internal granular coal is basically controlled within 35%, while the mass percentage of massive coal is basically above 50% in the whole region, and even in some areas, it can even approach 70%. Under the optimized scheme, the granular coal after blasting has its percentage of mass significantly reduced, while the mass percentage of lump coal is significantly increased.

D. EVALUATION OF BLASTING EFFECT

In order to analyze the global distribution of blockiness characteristics, the average mass percentage of each fragment type in the whole area under the original scheme and the optimization scheme is calculated, as shown in Table 10.

TABLE 10. Average size of coal mass in the whole region under original and optimized scheme.

Blasting plan	Average mass percentage /%		
	Granular coal	Massive coal	Large volume coal
Original plan	44.50	45.67	9.83
Optimization	29.87	60.65	9.48
Difference (optimized - original)	-14.63	14.98	-0.35

It can be seen from Table 10 that the percentage of granular coal mass can be reduced from 44.50% to 29.87% and the mass percentage of massive coal is increased from 46.57% to 60.65%, the amplitude reached 14.98%, while the mass percentage of large volume coal did not change much, and it could basically be controlled within 10%. Therefore, the blasting optimization scheme can effectively reduce the output of small-diameter granular coal, increase the output of lump coal in the range of 50-300mm, and meet the production needs of the Ha'erwusu open-pit coal mine.

V. CONCLUSION

According to the actual production of the Ha'erwusu open-pit mine, the characteristics of the coal seam blasting under the existing blasting parameters, combined with the mechanical test of the coal under the impact load, the relationship between the blasting parameters and the block distribution is established. The evaluation of the distribution characteristics and the optimization of the blasting parameters are proposed. The conclusions are as follows:

(1) The blasting division of single-hole blasting in coal seam is based on the theory of stress wave attenuation, and the relationship between the blasting load and the applied load of the indoor sample impact failure test is established. The coal rock with pressure between 0.13MPa and 2.0MPa is developed. The coal samples impact load test, through the decomposition sieve, obtained the block distribution characteristics of the coal rock sample under different impact pressure conditions.

(2) The impact crushing sample is divided into three groups according to the size of the fragments: large diameter, medium diameter and powder. The proportion of the three groups of fragments is determined according to the weight. Combining with the requirements of open-pit coal seam blasting on the proportion of lump coal, dust pollution control and cost control, the pressure range with good impact effect is determined as follows: $0.30\text{MPa} \leq P \leq 0.90\text{MPa}$.

(3) The image recognition system of coal seam blasting block degree was established by using MATLAB software. The distribution characteristics of coal and rock block between two blastholes in the coal seam blast zone of Ha'erwusu open-pit mine were analyzed.

(4) The existing coal seam blasting scheme was evaluated, and two sets of coal seam blasting parameters optimization schemes were proposed. The ANSYS/LS-DYNA numerical simulation method was used to verify the blasting area optimization rationalization after blasting parameters optimization. Through the optimization test of coal seam blasting, it is concluded that increasing the spacing of blasting holes and row spacing can effectively control the dust pollution of mine blasting and increase the lump coal rate.

(5) The research method can be used not only in the field of open-pit coal seam blasting, but also in the field of open-pit rock blasting. In addition, the specific methods of reducing large size coal blocks and the optimization of blasting parameters need to be further studied.

REFERENCES

[1] X. Lu, W. Zhou, X. Ding, X. Shi, B. Luan, and M. Li, "Ensemble learning regression for estimating unconfined compressive strength of cemented paste backfill," *IEEE Access*, vol. 7, pp. 72125–72133, 2019. doi: 10.1109/ACCESS.2019.2918177.

[2] C. Qi, A. Fourie, Q. Chen, and P. Liu, "Application of first-principles theory in ferrite phases of cemented paste backfill," *Minerals Eng.*, vol. 133, pp. 47–51, Mar. 2019.

[3] C. Qi, L. Liu, J. He, Q. Chen, L. Yu, and P. Liu, "Understanding cement hydration of cemented paste backfill: DFT study of water adsorption on tricalcium Silicate (111) Surface," *Minerals*, vol. 9, no. 4, p. 202, 2019. doi: 10.3390/min9040202.

[4] C. Qi and A. Fourie, "Cemented paste backfill for mineral tailings management: Review and future perspectives," *Minerals Eng.*, vol. 134, Art. no. 106025, 2019. doi: 10.1016/j.mineng.2019.106025.

[5] W. Li and R. S. Yang, "Application of loose blasting in fully-mechanized coal face crossing faults," *Adv. Mater. Res.*, vols. 838–841, pp. 1880–1883, Nov. 2014. doi: 10.4028/www.scientific.net/AMR.838-841.1880.

[6] S. Xiao, K. Li, X. Ding, and T. Liu, "Rock mass blastability classification using fuzzy pattern recognition and the combination weight method," *Math. Problems Eng.*, vol. 2015, 2015, Art. no. 724619. doi: 10.1155/2015/724619.

[7] A. Karami and S. Afiuni-Zadeh, "Sizing of rock fragmentation modeling due to bench blasting using adaptive neuro-fuzzy inference system and radial basis function," *Int. J. Mining Sci. Technol.*, vol. 22, no. 4, pp. 459–463, 2012.

[8] J. G. Fu, R. X. Luan, and Y. T. Zhang, "Roadway hard rock loose blasting by digging machine technique," *Appl. Mech. Mater.*, vols. 204–208, pp. 1758–1762, Oct. 2012. doi: 10.4028/www.scientific.net/AMM.204-208.1758.

[9] H.-B. Xia, Y. Xu, and H.-B. Wang, "Study on seismic wave propagation characteristic of deep-hole loose blasting in coal mine," in *Proc. 4th Int. Conf. Digit. Manuf. Automat.*, Jun. 2013, pp. 1290–1294. doi: 10.1109/ICDMA.2013.307.

[10] S. J. Qu, J. F. Liu, and W. Y. Xu, "Computer image automatic processing system for fragmentation distribution of blasting lumps and rocks," *Metal Mine*, vol. 42, no. 6, pp. 1–4, 2013. doi: 10.3969/j.issn.1001-1250.2013.06.001.

[11] B. Duan, H. Xia, and X. Yang, "Impacts of bench blasting vibration on the stability of the surrounding rock masses of roadways," *Tunnelling Underground Space Technol.*, vol. 71, pp. 605–622, Jan. 2018. doi: 10.1016/j.tust.2017.10.012.

[12] J. W. Wang, "The applied research of loose blasting technique in managing crushing accident of fully mechanized coal mining face," *Adv. Mater. Res.*, vols. 734–737, pp. 863–867, Aug. 2013. doi: 10.4028/www.scientific.net/AMR.734-737.863.

[13] I. T. Wang, "Numerical simulation and experimental validation of the Mach reflection effect of shock wave under ground surface blast," *J. Vibroeng.*, vol. 17, no. 3, pp. 1413–1423, 2015.

[14] S. Wang, E. A. Flores-Johnson, and L. Shen, "A technique for the elimination of stress waves overlapping in the split Hopkinson pressure bar," *Exp. Techn.*, vol. 41, no. 4, pp. 345–355, Apr. 2017.

[15] X. Ding, X. Lu, W. Zhou, X. Shi, B. Luan, and M. Li, "Blasting impact simulation test and fragmentation distribution characteristics in an open-pit mine," *Shock Vib.*, vol. 2019, 2019, Art. no. 4080274. doi: 10.1155/2019/4080274.

[16] J. E. Field, S. M. Walley, W. G. Proud, H. T. Goldrein, and C. R. Siviour, "Review of experimental techniques for high rate deformation and shock studies," *Int. J. Impact Eng.*, vol. 30, no. 7, pp. 725–775, 2004.

[17] R. P. Dai, X. B. Guo, Q. M. Gong, C. J. Pu, and Z. C. Zhang, "SHPB test on blasting damage protection of tunnel surrounding rock," *Rock Soil Mech.*, vol. 32, no. 1, pp. 77–83, 2011.

[18] J. Shi, X. Guo, Z. Xiao, and Z. Zhang, "Experimental study on ultrasonic velocity and damage properties of rock under dynamic loading," *Mining Res. Develop.*, vol. 25, no. 6, pp. 27–29, 2005.

[19] H. Guo, L. J. Guo, D. N. Zhang, X. Liu, Y. D. Qi, and Y. Gao, "Application of hopkinson compressive bar experiment in blasting," (in Chinese), *Mod. Mining*, vol. 31, no. 3, pp. 174–176, 2015.

[20] Z. Y. Ti, "Summary of methods after estimation of fragment size distribution from blasting in opencast mining," *J. Fuxin Mining Inst.(Natural Sci.)*, vol. 13, no. 2, pp. 38–43, 1994.

[21] L. H. Jin, H. Luo, X. Z. Zheng, S. Chen, and Q. X. Liang, "Fractal expression of dust volume dispersion in bench blasting in open air," *China Saf. Sci. J.*, vol.26, no. 8, pp. 139–144, 2016.

[22] D. F. Yi, "The study of automatic analysis model to the size distribution of piled ore after blowing up," M.S. thesis, Liaoning Tech. Univ., Fuxin, China, 2004.

[23] J.-H. Han and J.-J. Song, "Statistical estimation of blast fragmentation by applying stereophotogrammetry to block piles," *Int. J. Rock Mech. Mining Sci.*, vol. 68, pp. 150–158, Jun. 2014.

[24] C. Arango and C. A. Morales, "Comparison between multicopter UAV and total station for estimating stockpile volumes," *Int. Arch. Photogramm., Remote Sens. Spatial Inf. Sci.*, vol. 40, no. 1, pp. 131–135, 2015.

[25] Y. Liu, "Application technology and development direction of digital image processing," *China Comput. Commun.*, vol. 14, no. 5, pp. 149–150, 2018.

[26] A. Delorme and S. Makeig, "EEGLAB: An open source toolbox for analysis of single-trial EEG dynamics including independent component analysis," *J. Neurosci. Methods*, vol. 134, no. 1, pp. 9–21, Mar. 2004.

[27] X. W. Song, Z.-Y. Dong, X.-Y. Long, S.-F. Li, X.-N. Zuo, C.-Z. Zhu, Y. He, C.-G. Yan, and Y.-F. Zang, "REST: A toolkit for resting-state functional magnetic resonance imaging data processing," *PLoS ONE*, vol. 6, no. 9, 2011, Art. no. e25031. doi: 10.1371/journal.pone.0025031.

[28] B. E. Treeby and B. T. Cox, "k-Wave: MATLAB toolbox for the simulation and reconstruction of photoacoustic wave fields," *J. Biomed. Opt.*, vol. 15, no. 2, Mar. 2010, Art. no. 021314. doi: 10.1117/1.3360308.

[29] V. Willenbockel, J. Sadr, D. Fiset, G. O. Horne, F. Gosselin, and J. W. Tanaka, "Controlling low-level image properties: The SHINE toolbox," *Behav. Res. Methods*, vol. 42, no. 3, pp. 671–684, Aug. 2010.

[30] J. Yang, W. Yin, Y. Zhang, and Y. Wang, "A fast algorithm for edge-preserving variational multichannel image restoration," *SIAM J. Imag. Sci.*, vol. 2, no. 2, pp. 569–592, 2009.

[31] *General Administration of Quality Supervision, Inspection and Quarantine of the People's Republic of China. GB 6722-2014, Safety regulations for blasting*. National Standards of the People's Republic of China, Beijing, China, 2014.

[32] D. Z. Liu and S. C. Yang, *Practical Manual for Engineering Blasting*, Beijing, China: Metallurgical Industry Press, 2003.

[33] X. Y. Wei, Z. Y. Zhao, and J. Gu, "Numerical simulations of rock mass damage induced by underground explosion," *Int. J. Rock Mech. Mining Sci.*, vol. 46, no. 7, pp. 1206–1213, Oct. 2009.

[34] W. Y. Meng, G. C. Xu, J. Q. Li, G. C. Xu, J. W. Guo, and W. Zhao, "Numerical simulation and experimental research of icicles under the single point of blasting in the yellow river," *Appl. Mech. Mater.*, vols. 501–504, pp. 2020–2025, Jan. 2014. doi: 10.4028/www.scientific.net/AMM.501-504.2020.

[35] D. J. Shen, Y. F. Si, Y. W. Cui, and S. X. Wu, "Three-dimensional finite element analysis of dispersion effect in SHPB tests," in *Proc. 3rd Int. Conf. Earthquake Eng.*, 2004, pp. 388–392.

[36] D. F. Su, D. D. Zheng, and L. G. Zhao, "Experimental Study and Numerical Simulation of Dynamic Stress-Strain of Directional Blasting with Water Jet Assistance," *Shock Vib.*, vol. 2019, Mar. 2019, Art. no. 1659175. doi: 10.1155/2019/1659175.
[37] H. C. Li, "The study of the rock RHT model and to determine the values of main parameters," Ph.D. dissertation China Univ. Mining Technol., Beijing, China, 2016.
[38] F. Liu, S. Gao, H. Han, Z. Tian, and P. Liu, "Interference reduction of high-energy noise for modal parameter identification of offshore wind turbines based on iterative signal extraction," *Ocean Eng.*, vol. 183, pp. 372–383, Jul. 2019.

XIAOHUA DING was born in Lianyungang, Jiangsu, China. He received the B.S., M.S., and Ph.D. degrees in mining engineering from the China University of Mining Technology, Xuzhou, China, in 2008, 2011, and 2014, respectively, where he has been a Lecture with the School of Mines, since 2014. He has authored two books and more than ten articles. He holds two patents. His research interests include surface mining, blasting engineering and dust control in open-pit mines.

WEI ZHOU was born in Yancheng, Jiangsu, China, in 1982. He received the B.S. and Ph.D. degrees in mining engineering from the China University of Mining and Technology, in 2005 and 2010, respectively, where he was a Lecturer with the School of Mines from 2010 to 2012. From 2013 to 2016, he was an Associate Professor. Since 2017, he has been a Professor with the School of Mines, China University of Mining and Technology. He has authored two books and more than 50 articles. He holds five patents. His research interests include surface mining, the mechanical properties of soil-rock mixture, land reclamation, and green mining.

Prof. Zhou was a member of the Society of Mining Professors.

XIANG LU was born in Zhangjiakou, Hebei, China. He received the B.S. degree in mining engineering from the China University of Mining Technology, Xuzhou, China, in 2016, where he is currently pursuing the Ph.D. degree in mining engineering. His research interests include mining engineering, open-pit mining, green mining and machine learning and application in mining area, especially in the exploration of interdisciplinary fields of computer and mine.

MING LI was born in Linyi, Shandong, China. He received the B.S. and Ph.D. degrees in engineering mechanics from the China University of Mining Technology, Xuzhou, China, in 2009 and 2014, respectively, where he has been a Research Associate Lecture with the State Key Laboratory for Geomechanics and Deep Underground Engineering, since 2015. He has authored one book and more than five articles. He holds our patents. His research interests include rock mechanics, rock impact, and blasting engineering.

EBELIA MANDA was born in Zambia. She is currently pursuing the Ph.D. degree in mining engineering with the China University of Mining and Technology, Xuzhou, China. She is also a Mining Engineer and a Lecturer with Copperbelt University, Zambia. She has 8 years' work experience in both underground and surface mining. Her research interests include blasting, environment evaluation, and intelligent mining.

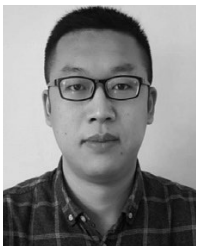

XUYANG SHI was born in Shijiazhuang, Hebei, China. He received the B.S. degree in engineering mechanics from the China University of Mining Technology, Xuzhou, China, in 2012, where he is currently pursuing the Ph.D. degree in mining engineering. His research interests include open-pit mining, seepage properties of rock, and soil-rock mixture, especially in the exploration of interdisciplinary fields of computer and mine.

BOYU LUAN was born in Hulun Buir, Inner Mongolia, China. He received the B.S. degree in mining engineering from the China University of Mining Technology, Xuzhou, China, in 2017, where he is currently pursuing the Ph.D. degree. His research interests include open-pit mining, dust control, and mining system engineering, especially in the exploration of interdisciplinary fields of computer and mine.

CHONGCHONG QI received the B.S. degree in mining engineering from the China University of Mining Technology, Xuzhou, China, and the Ph.D. degree from The University of Western Australia. He is currently a Professor with Central South University, Changsha, China. He has authored more than 30 articles published in reputed international journals. His research interests include cemented paste backfill, dust control, and environment protection in the mining industry.